

The Reading Palaeofire database: an expanded global resource to document changes in fire regimes from sedimentary charcoal records

Sandy P. Harrison^{1,2}, Roberto Villegas-Diaz¹, Esmeralda Cruz-Silva¹, Daniel Gallagher^{2,3}, David Kesner^{1,2}, Paul Lincoln^{1,2}, Yicheng Shen¹, Luke Sweeney^{1,2}, Daniele Colombaroli^{2,3}, Adam Ali⁴, Chéïma Barhoumi⁵, Yves Bergeron^{6,7}, Tatiana Blyakharchuk⁸, Přemysl Bobek⁹, Richard Bradshaw¹⁰, Jennifer L. Clear¹¹, Sambor Czerwiński¹², Anne-Laure Daniau¹³, John Dodson^{14,15}, Kevin J. Edwards^{16,17}, Mary E. Edwards¹⁸, Angelica Feurdean¹⁹, David Foster²⁰, Konrad Gajewski²¹, Mariusz Gałka²², Michelle Garneau²³, Thomas Giesecke²⁴, Graciela Gil Romera^{25,26}, Martin P. Girardin²⁷, Dana Hoefler²⁸, Kangyou Huang²⁹, Jun Inoue³⁰, Eva Jamrichová⁹, **Nauris** Jasiunas³¹, Wenying Jiang³², Gonzalo Jiménez-Moreno³³, Monika Karpińska-Kołaczek¹², Piotr Kołaczek¹², Niina Kuosmanen³⁴, Mariusz Lamentowicz³⁵, Martin Lavoie³⁶, Fang Li³⁷, Jianyong Li³⁸, Olga Lisitsyna^{39,40}, José Antonio López-Sáez⁴¹, Reyes Luelmo-Lautenschlaeger⁴¹, Gabriel Magnan²³, Eniko Katalin Magyari⁴², Alekss Maksims⁴³, Katarzyna Marcisz¹², Elena Marinova⁴⁴, Jenn Marlon⁴⁵, Scott Mensing⁴⁶, Joanna Mirosław-Grabowska⁴⁷, Wyatt Oswald^{20,48}, Sebastián Pérez-Díaz⁴⁹, Ramón Pérez-Obiol⁵⁰, Sanna Piilo⁵¹, Anneli Poska^{39,52}, Xiaoguang Qin⁵³, Cécile C. Remy⁵⁴, Pierre **J.H.** Richard⁵⁵, Sakari Salonen³⁴, Naoko Sasaki⁵⁶, Hieke Schneider⁵⁷, William Shotyk⁵⁸, Migle Stancikaite⁵⁹, Dace Šteinberga⁴³, Normunds Stivrins^{31,39,60}, Hikaru Takahara⁶¹, Zhihai Tan⁶², Liva Trasune^{31,34}, Charles E. Umbanhowar⁶³, Minna Väiliranta⁵¹, Jüri Vassiljev³⁹, Xiayun Xiao⁶⁴, Qinghai Xu⁶⁵, Xin Xu³⁷, Edyta Zawisza⁶⁶, Yan Zhao⁶⁷, Zheng Zhou²⁹, **Jordan Paillard**⁶⁸

- 1: School of Archaeology, Geography & Environmental Science, Reading University, Whiteknights, Reading, RG6 6AH, UK
- 2: Leverhulme Centre for Wildfires, Environment and Society, Imperial College London, South Kensington, London, SW7 2BW, UK
- 3: Department of Geography, Royal Holloway, University of London, Egham, TW20 0 SS, UK
- 4: University de Montpellier, Institut des Sciences de l'Evolution (CNRS, IRD, EPHE), France
- 5: Department of Palynology and Climate Dynamics, Albrecht-von-Haller Institute for Plant Sciences, University of Göttingen, Untere Karspüle 2, 37073 Göttingen, Germany
- 6: Forest Research Institute (IRF), Université du Québec en Abitibi-Témiscamingue (UQAT), Rouyn-Noranda, QC, Canada J9X 5E4
- 7: Department of Biological Sciences, Université du Québec à Montréal (UQAM), Montréal, QC, Canada H3C 3P8
- 8: Institute of Monitoring of Climatic and Ecological Systems of Siberian branch of Russian Academy of Sciences (IMCES SB RAS), Tomsk, 634055, Russia
- 9: Institute of Botany, Czech Academy of Sciences, Lidická 25/27, 602 00 Brno, Czech Republic

- 10: Geography and Planning, University of Liverpool, Liverpool, L69 7ZT, UK
- 11: Department of Geography and Environmental Science, Liverpool Hope University, Taggart Street, Childwall, Liverpool, L16 9JD, UK
- 12: Climate Change Ecology Research Unit, Faculty of Geographical and Geological Sciences, Adam Mickiewicz University, Poznań, Bogumiła Krygowskiego 10, 61-680 Poznań, Poland
- 13: Environnements et Paléoenvironnements Océaniques et Continentaux (EPOC), Unité Mixte de Recherche (UMR) 5805, Centre National de la Recherche Scientifique (CNRS), Université de Bordeaux, 33615 Pessac, France
- 14: Institute of Earth Environment, Chinese Academy of Sciences, Keji 1st Rd, Yanta District, Xi'an, Shaanxi, China
- 15: School of Earth, Atmospheric and Life Sciences, University of Wollongong, Wollongong, NSW 2500, Australia
- 16: Department of Geography & Environment and Archaeology, University of Aberdeen, Aberdeen AB24 3UX, UK
- 17: McDonald Institute for Archaeological Research and Scott Polar Research Institute, University of Cambridge, Cambridge, UK
- 18: School of Geography and Environmental Science, University of Southampton, Southampton SO17 1BJ, UK
- 19: Department of Physical Geography, Goethe University, Altenhöferallee 1, 60438 Frankfurt am Main, Germany
- 20: Harvard Forest, Harvard University, Petersham MA 01366 USA
- 21: Département de Géographie, Environnement et Géomatique, Université d'Ottawa, Ottawa, ON, K1N6N5 Canada
- 22: University of Lodz, Faculty of Biology and Environmental Protection, Department of Biogeography, Paleocology and Nature Protection, 1/3 Banacha Str., 90-237 Lodz, Poland
- 23: GEOTOP Research Center, Université du Québec à Montréal, Montréal QC, H2X 3Y7, Canada
- 24: Department of Physical Geography, Faculty of Geosciences, Utrecht University, Netherlands
- 25: Instituto Pirenaico de Ecología-CSIC, Avda. Montañana 1005, 50059, Zaragoza, Spain
- 26: Plant Ecology & Geobotany, Karl-Von-Frisch-Straße 8, Philipps University of Marburg, Marburg
- 27: Natural Resources Canada, Canadian Forest Service, Laurentian Forestry Centre, Quebec City, QC, Canada
- 28: Senckenberg Research Station of Quaternary Palaeontology, Am Jakobskirchhof 4, 99423 Weimar, Germany
- 29: School of Earth Sciences and Engineering, Sun Yat-sen University, Zhuhai 519082, China
- 30: Department of Geosciences, Graduate School of Science, Osaka City University, Osaka, Japan
- 31: Department of Geography, University of Latvia, Jelgavas iela 1, Riga, LV-1004, Latvia
- 32: Key Laboratory of Cenozoic Geology and Environment, Institute of Geology and Geophysics, Chinese Academy of Sciences, Beijing, China
- 33: Departamento de Estratigrafía y Paleontología, Facultad de Ciencias, Universidad de Granada, Avda. Fuente Nueva S/N, 18002 Granada, Spain
- 34: Department of Geosciences and Geography, University of Helsinki, P.O.Box 64, FI-00014, Helsinki, Finland
- 35: Faculty of Geographical and Geological Sciences, Adam Mickiewicz University in Poznan, Bogumiła Krygowskiego 10, 61-680 Poznan, Poland

- 36: Département de géographie, Université Laval, Québec, Canada
- 37: International Center for Climate and Environment Sciences, Institute of Atmospheric Physics, Chinese Academy of Sciences, Beijing, China
- 38: Shaanxi Key Laboratory of Earth Surface System and Environmental Carrying Capacity, College of Urban and Environmental Sciences, Northwest University, Xi'an 710127, China
- 39: Department of Geology, Tallinn University of Technology, Ehitajate tee 5, 19086 Tallinn, Estonia
- 40: Russian State Agrarian University, Timiryazevskaya st., 49, 127550, Moscow, Russia
- 41: Environmental Archaeology Research Group, Institute of History, CSIC, Madrid, Spain
- 42: Department of Environmental and Landscape Geography, ELKH-MTM-ELTE Research Group for Paleontology, Eotvos Lorand university, 1117 Budapest, Pazmany Peter stny 1/c, Budapest, Hungary
- 43: Department of Geology, University of Latvia, Jelgavas iela 1, Riga, LV-1004, Latvia
- 44: Laboratory for Archaeobotany, State Office for Cultural Heritage Baden-Württemberg, Fischersteig 9, 78343 Geienhofen-Hemmenhofen, Germany
- 45: Yale School of the Environment, New Haven, Connecticut 06511, USA
- 46: Department of Geography, University of Nevada Reno, 1664 N Virginia St, Reno, NV 89557, USA
- 47: Institute of Geological Sciences, Polish Academy of Sciences, Warsaw, Poland
- 48: Marlboro Institute for Liberal Arts and Interdisciplinary Studies, Emerson College, Boston MA 02116 USA
- 49: Department of Geography, Urban and Regional Planning, University of Cantabria, Santander, Spain
- 50: Unitat de Botànica, Facultat de Biociències, Universitat Autònoma de Barcelona, Cerdanyola del Vallès, 08193 Barcelona, Spain
- 51: Environmental Change Research Unit (ECRU), Ecosystems, Environment Research Programme, Faculty of Biological and Environmental Sciences, Viikinkaari 1, P.O. Box 65, 00014 University of Helsinki, Finland
- 52: Department of Physical Geography and Ecosystem Science, Lund University, Lund, Sweden
- 53: Key Laboratory of Cenozoic Geology and Environment, Institute of Geology and Geophysics, Chinese Academy of Sciences, No.19 Beitucheng West RD, Beijing, 100029, China
- 54: Institut für Geographie, Universität Augsburg, 86135 Augsburg, Germany
- 55: Département de géographie, Complexe des sciences, Université de Montréal, Montréal, H2V 0B3, Canada
- 56: Graduate School of Life and Environmental Sciences, Kyoto Prefectural University, 1-5 Hangi-cho, Shimogamo, Sakyo-ku, Kyoto 606-8522, Japan
- 57: Institut für Geographie, Friedrich-Schiller-Universität Jena, Löbdergraben 32, 07743 Jena, Germany
- 58: Department of Renewable Resources, University of Alberta, 348B South Academic Building, Edmonton, Alberta T6G 2H1, Canada
- 59: Institute of Geology and Geography, Nature Research Centre, Akademijos Str. 2, LT-08412, Vilnius, Lithuania
- 60: Latvian Institute of History, University of Latvia, Kalpaka blv. 4, Riga, LV-1050, Latvia
- 61: Graduate School of Agriculture, Kyoto Prefectural University, Shimogamo, Sakyo-ku, 1-5, Hangi-cho, 606-8522 Kyoto, Japan
- 62: School of Environment and Chemistry Engineering, Xi'an Polytechnic University, Xi'an, Shaanxi 710048, China

- 63: Departments of Biology and Environmental Studies, St Olaf College, 1520 St Olaf Ave, Northfield, MN 55057, USA
- 64: State Key Laboratory of Lake Science and Environment, Nanjing Institute of Geography and Limnology, Chinese Academy of Sciences, Nanjing 210008, China
- 65: College of Resources and Environment Sciences, Hebei Normal University, Shijiazhuang 050024, China
- 66: Institute of Geological Sciences, Polish Academy of Sciences, Twarda 51/55, 00-818 Warsaw, Poland
- 67: Institute of Geographic Sciences and Natural Resources Research, Chinese Academy of Sciences, Beijing 100101, China
- 68: Département de Géographie, Université de Montréal, C.P. 6128, Succ. Centre-Ville Montréal Québec, H3C 3J7, Canada

Corresponding author: Sandy P. Harrison, s.p.harrison@reading.ac.uk

Ms for *Earth System Science Data*

1 **Abstract**

2 Sedimentary charcoal records are widely used to reconstruct regional changes in fire regimes
3 through time in the geological past. Existing global compilations are not geographically
4 comprehensive and do not provide consistent metadata for all sites. Furthermore, the age
5 models provided for these records are not harmonised and many are based on older calibrations
6 of the radiocarbon ages. These issues limit the use of existing compilations for research into
7 past fire regimes. Here, we present an expanded database of charcoal records, accompanied by
8 new age models based on recalibration of radiocarbon ages using INTCAL2020 and Bayesian
9 age-modelling software. We document the structure and contents of the database, the
10 construction of the age models, and the quality control measures applied. We also record the
11 expansion of geographical coverage relative to previous charcoal compilations and the
12 expansion of metadata that can be used to inform analyses. This first version of the Reading
13 Palaeofire Database contains 1676 records (entities) from 1480 sites worldwide. The database
14 is available from <https://doi.org/10.17864/1947.000345>.

15 1. Introduction

16 Wildfires have major impacts on terrestrial ecosystems (Bond et al., 2005; Bowman et al.,
17 2016; He et al., 2019; Lasslop et al., 2020), the global carbon cycle (Li et al., 2014; Arora and
18 Melton, 2018; Pellegrini et al., 2018; Lasslop et al., 2019), atmospheric chemistry (van der
19 Werf et al., 2010; Voulgarakis and Field, 2015; Sokolik et al., 2019) and climate (Randerson
20 et al., 2006; Li et al., 2017; Harrison et al., 2018; Liu et al., 2019). Although the climatic,
21 vegetation and anthropogenic controls on wildfires are relatively well understood (e.g.
22 Harrison et al., 2010; Bistinas et al., 2014; Knorr et al., 2016; Forkel et al., 2017; Li et al.,
23 2019), recent years have seen wildfires occurring in regions where they were historically rare
24 (e.g. northern Alaska, Greenland, northern Scandinavia: [Evangelidou et al., 2019](#); [Hayasaka,](#)
25 [2021](#)) and an increase in fire frequency and severity in more fire-prone regions (e.g. California,
26 the circum-Mediterranean, eastern Australia; e.g. [Abatzoglou and Williams, 2016](#); [Dutta et al.,](#)
27 [2016](#); [Williams et al., 2019](#); [Nolan et al., 2020](#)). It is useful to look at the pre-industrial era
28 (conventionally defined as pre 1850 CE) to understand whether these events are atypical. The
29 pre-industrial past also provides an opportunity to characterise fire regimes before
30 anthropogenic influences, both in terms of ignitions and fire suppression, became important.

31 Ice-core records provide a global picture of changes in wildfire in the geologic past (Rubino et
32 al., 2016). However, wildfires exhibit considerable local to regional variability because of the
33 spatial heterogeneity of the various factors controlling their occurrence and intensity ([Bistinas](#)
34 [et al., 2014](#); [Andela et al., 2019](#); [Forkel et al., 2019](#)). Thus, it is useful to use information that
35 can provide a picture of regional changes through time. Charcoal, preserved in lake, peat or
36 marine sediments, can provide a picture of such changes ([Clark and Patterson, 1997](#); [Conedera](#)
37 [et al., 2009](#)). The wildfire regime can be characterised from sedimentary charcoal records
38 through total charcoal abundance per unit of sediment, which can be considered as a measure
39 of the total biomass burned (e.g. Marlon et al., 2006) or by the presence of peaks in charcoal
40 accumulation which, in records with sufficiently high temporal resolution, can indicate
41 individual episodes of fire (e.g. Power et al., 2006).

42 The Global Palaeofire Working Group (GPWG) was established in 2006 to coordinate the
43 compilation and analysis of charcoal data globally, through the construction of the Global
44 Charcoal Database (GCD: Power et al., 2008). The GPWG was initiated by the International
45 Geosphere-Biosphere Programme (IGBP) Fast-Track Initiative on Fire and subsequently

46 recognised as a working group of the Past Global Changes (PAGES) Project in 2008. There
47 have now been several iterations of the GCD (Power et al., 2008; Power et al., 2010; Daniau
48 et al., 2012; Blarquez et al., 2014; Marlon et al., 2016), which since 2020 has been managed
49 by the International Palaeofire Network as the Global Palaeofire Database (GPD;
50 <https://paleofire.org>). The GCD has been used to examine changes in fire regimes over the past
51 two millennia (Marlon et al., 2008), during the current interglacial (Marlon et al., 2013), on
52 glacial-interglacial timescales (Power et al., 2008; Daniau et al., 2012; Williams et al., 2015)
53 and in response to rapid climate changes (Marlon et al., 2009; Daniau et al., 2010), as well as
54 to examine regional fire histories (e.g. Mooney et al., 2011; Vanni re et al., 2011; Marlon et
55 al., 2012; Power et al., 2013; Feurdean et al., 2020). However, there are a number of limitations
56 to the use of the GCD for analyses of palaeofire regimes. Firstly, the database does not include
57 many recently published records and needs to be updated. Secondly, there are inconsistencies
58 among the various versions of the database including duplicated and/or missing sites,
59 differences in the metadata included for each site or record, and missing metadata **and dating**
60 **information** for some sites or records. Perhaps most crucially, the age models included in the
61 database were made at different times, using different radiocarbon calibration curves, and using
62 different age-modelling methods. The disparities between the archived age models preclude a
63 detailed comparison of changes in wildfire regimes across regions.

64 Here, we present an expanded database of charcoal records (the Reading Palaeofire Database,
65 RPD), accompanied by new age models based on recalibration of radiocarbon ages using
66 INTCAL2020 (Reimer et al., 2020) and using a consistent Bayesian approach (BACON:
67 Blaauw. et al., 2021) to age-model construction. **However, we have retained the original age**
68 **models for all the sites for comparison and to allow the user to choose a preferred age model.**
69 **The RPD is designed to facilitate regional analyses of fire history; it is not designed as a**
70 **permanent repository.** We document the structure and contents of the database, the construction
71 of the new age models, the expanded metadata available, and the quality control measures
72 applied to check the data entry. We also document the expansion of the geographic and
73 temporal coverage, and in the availability of metadata, relative to previous GCD compilations.

74 2. Data and Methods

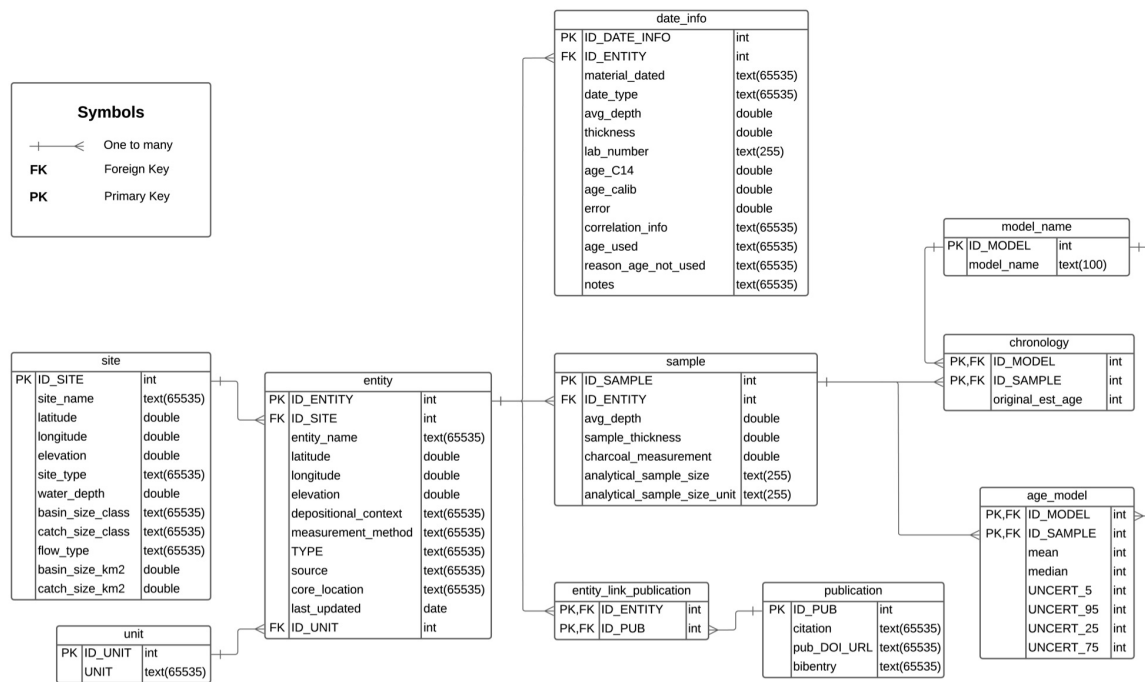
75 2.1. Compilation of data

76 The database contains sedimentary charcoal records, metadata to facilitate the interpretation of
77 these records, and information on the dates used to construct the original age model for each
78 record. Some records were obtained from the GCD. There are multiple versions of the GCD
79 which differ in terms of the sites and the types of metadata included. We compared the GCDv3
80 (Marlon et al., 2016), GCDv4 (Blarquez, 2018) and GCD webpage versions
81 (<http://paleofire.org>) and extracted a single unique version of each site and entity across the
82 three versions. Where sites or entities were duplicated in different versions of the GCD, we
83 used the latest version. Missing metadata and dating information for these records were
84 obtained from the literature or from the original data providers. Some sites in the GCD were
85 represented by both concentration data and the same data expressed as influx (i.e. concentration
86 per year) from the same samples; because influx calculations are time dependent, we have only
87 retained concentration data for such sites to allow for future improvements to age models.
88 Influx can be easily computed using data available in the RPD. **We also removed duplicates**
89 **where the GCD contained both raw data and concentration data from the same entity.** We
90 extracted published charcoal records ~~that do not appear in any version of the GCD~~ from public
91 repositories, specifically PANGAEA (<https://www.pangaea.de/>), NOAA National Centre for
92 Environmental Information (<https://www.ncdc.noaa.gov/data-access/paleoclimatology-data>),
93 the Neotoma Paleoecology Database (<https://www.neotomadb.org/>), the European Pollen
94 Database (<http://www.europeanpollendatabase.net/index.php>) and the Arctic Data Centre
95 (<https://arcticdata.io/catalog/>); **if these records were also in the GCD we replaced the GCD**
96 **version.** Additional charcoal data, dating information and metadata were provided directly by
97 the authors. All the records in the current version of the database are listed in the Supplementary
98 Information (SI Table 1).

99 2.2 Structure of the database

100 The data are stored in a relational database (MySQL), which consists of 10 linked tables,
101 specifically "site", "entity", "sample", "date info", "unit", "entity link publication",
102 "publication", "chronology", "age model", and "model name". Figure 1 shows the relationships
103 between these tables. A description of the structure and content of each of the tables is given

104 below, and more detailed information about individual fields is given in the Supplementary
 105 Material (SI Table 2).



106

107 *Figure 1. Entity-relation diagram showing the structure of the database, individual tables and*
 108 *their contents, and the nature of the relationships between the component tables. One-to-many*
 109 *linkages indicate that it is possible to have several entries on one table linked to a single entry*
 110 *in another table. The database uses both primary and foreign keys. The primary key ensures*
 111 *that data included in a specific field is unique. The foreign key refers to the field in a table*
 112 *which is the primary key of another table and ensures that there is a link between these tables.*

113 **2.2.1 Site metadata (table name: site)**

114 A site is defined as the hydrological basin from which charcoal records have been obtained
 115 (Table 1). There may be several charcoal records from the same site, for example where
 116 charcoal records have been obtained on central and marginal cores from the same lake or where
 117 there is a lake core and additional cores from peatlands and/or terrestrial deposits (e.g. small
 118 hollows, soils) within the same hydrological basin. A site may therefore be linked to several
 119 charcoal records, where each record is treated as a separate entity. The site table contains basic
 120 metadata about the basin, including site ID, site name, latitude, longitude, elevation, site type,
 121 and maximum water depth. The site names are expressed without diacritics to facilitate

122 database querying and subsequent analyses in programming languages that do not handle these
 123 characters. Latitude and longitude are given in decimal degrees, truncated to six decimal places
 124 since this gives an accuracy of <1m at the equator. Broad categories of site type are
 125 differentiated (e.g. terrestrial, lacustrine, marine), with subdivisions according to geomorphic
 126 origin (e.g. lakes are recorded according to whether they are e.g. fluvial, glacial or volcanic in
 127 origin). In addition to coastal salt marshes and estuaries, we include a generic coastal category
 128 for all types of sites that lie within the coastal zone and the hydrology may therefore have been
 129 affected by changes in sea level. Wherever possible, the size of the basin and the catchment
 130 are recorded (in km²) but if accurate quantified information is not available the basin and
 131 catchment size are recorded by size classes. The site table also contains information on whether
 132 the lake or peatland is hydrologically closed or has inflows and outflows, which can affect the
 133 source, quantity and preservation of charcoal in the sediments. **A complete listing of the sites
 134 and entities in the RPD is given in Table S1. A list of the valid choices for fields that are
 135 selected from a pre-defined list (e.g. site type) is given in Table S2.**

136 Table 1 Definition of the site table.

Field name	Definition	Data type	Constraints / Notes
ID_SITE	Unique identifier for each site	Unsigned integer	positive integer
site_name	Site name as given by original authors or as defined by us where there was no unique name given to the site	Text	Required
latitude	Latitude of the sampling site, given in decimal degrees, where N is positive and S is negative	Double	Numeric value between -90 and 90
longitude	Longitude of the sampling site in decimal degrees, where E is positive and W is negative	Double	Numeric value between -180 and 180
elevation	Elevation of the sampling site in metres above (+) or below (-) sea level	Double	None

site_type	Information about type of site (e.g. lake, peatland, terrestrial)	Text	Selected from pre-defined list
water_depth	Water depth of the sampling site in metres	Double	None
flow_type	Indication of whether there is inflow and/or outflow from the sampled site	Text	Selected from pre-defined list
basin_size_km2	Size of sampled site (e.g. lake or bog) in km ²	Double	None
catch_size_km2	Size of hydrological catchment in km ²	Double	None
basin_size_class	Categorical estimate of basin size	Text	Selected from pre-defined list
catch_size_class	Categorical estimate of hydrological catchment size	Text	Selected from pre-defined list

137 **2.2.2 Entity metadata (table name: entity)**

138 This table provides metadata for each individual entity (Table 2). In addition to distinguishing
139 multiple cores from the same basin as separate entities, we also distinguish different size
140 classes of charcoal from the same core when these data are available. Different charcoal size
141 classes from the same core are also treated as separate entities in the database. **However, we**
142 **have removed duplicates where the same record was expressed in different ways (e.g. as both**
143 **raw counts and concentration, or as concentration and influx) to avoid confusion and mistakes**
144 **when subsequently processing these data. The RPD contains raw data wherever possible,**
145 **concentration data when the raw data is not available, and only includes influx data if neither**
146 **are available.** When specific cores were given distinctive names in the original publication or
147 by the original author, we include this information in the entity name for ease of cross-
148 referencing. The entity metadata include information that can be used to interpret the charcoal
149 records, including depositional context, core location, measurement method, and measurement
150 unit. There is no standard measurement unit for charcoal, and in fact, there are **>100 different**
151 **units** employed in the database. For convenience, there is a link table to the measurement units
152 (table name: unit). In addition, the entity table provides the source from which the charcoal
153 data were obtained, including whether these data are from a version of the GCD, a data

154 repository or were provided by the original author, and an indication of when the record was
 155 last updated. A list of the valid choices for fields that are selected from a pre-defined list (e.g.
 156 depositional context) is given in Table S2. A list of the charcoal measurement units currently
 157 in use in the RPD is given in Table S3.

158 Table 2 Definition of the entity table.

Field name	Definition	Data type	Constraints / Notes
ID_ENTITY	Unique identifier for each entity	Unsigned integer	Positive integer
ID_SITE	Refers to unique identifier for each site (as given in site table)	Unsigned integer	Auto-numeric, foreign key of the site table, a positive integer
entity_name	Name of entity, where an entity may be a separate core from the site or a separate type of measurement on the same core	Text	Required
latitude	Latitude of the entity, given in decimal degrees, where N is positive and S is negative	Double	A numeric value between -90 and 90
longitude	Longitude of the entity, given in decimal degrees, where E is positive and W is negative	Double	A numeric value between -180 and 180
elevation	Elevation of the sampling site, in metres above (+) or below (-) sea level	Double	None
depositional_context	Type of sediment sampled for charcoal	Text	Selected from pre-defined list
measurement_method	Method used to measure the amount of charcoal	Text	Selected from pre-defined list
TYPE	The unit type of the measured charcoal values (e.g. concentration, influx)	Text	Selected from pre-defined list

source	Source of charcoal data	Text	Selected from pre-defined list
core_location	Location of the entity within the site (e.g. central core or marginal core)	Text	Selected from pre-defined list
last_updated	Date when the entity or its linked data was last updated	Date	In format YYYY/mm/dd
ID_UNIT	Unique identifier for measurement unit (as in unit table)	Unsigned integer	Auto-numeric, foreign key of the unit table, a positive integer

159

160 **2.2.3 Sample metadata and data (table name: sample)**

161 The sample table provides information on the average depth in the core or profile and the
162 thickness of the sample on which charcoal was measured. The thickness measurements relate
163 to the total thickness of the charcoal sample and provide an indication of whether the sampling
164 was contiguous downcore. The sample table also provides information on the sample volume
165 and the quantity of charcoal present. **The charcoal measurement units have been standardised
166 by converting units expressed as multiples (e.g. fragments x100) back to the whole numbers
167 and by converting units expressed in mg or kg to g. As a result, the values in the RPD may
168 apparently differ from published values.**

169 Table 3 Definition of the sample table.

Field name	Definition	Data type	Constraints / Notes
ID_SAMPLE	Unique identifier for each charcoal sample	Unsigned integer	Auto-numeric, primary key, a positive integer
ID_ENTITY	Unique identifier for the entity (as in entity table)	Unsigned integer	Auto-numeric, foreign key of the entity table, a positive integer

avg_depth	Average sampling depth, in metres	Double	None
sample_thickness	Sample thickness, in metres	Double	None
charcoal_measurement	Quantity of charcoal measured in the sample	Double	None
analytical_sample_size	Total amount of sediment sampled	Text	255 characters maximum length
analytical_sample_size_unit	Units used for the sampling	Text	255 characters maximum length

170

171 **2.2.4 Dating information (table name: date info)**

172 This table provides information about the dates available for each entity that can be used to
173 construct an age model. We include information about the age of the core top for records that
174 were known to be actively accumulating sediment at the time of collection. In addition to
175 radiometric dates, we include information about the presence of tephras (either dated at the site
176 or independently dated elsewhere) and stratigraphic events that can be used to establish
177 correlative ages (e.g. changes in the pollen assemblage that are dated in other cores from the
178 region, or evidence of known fires in the catchment). Wherever possible the name of a tephra
179 is given, to facilitate the use of subsequent and more accurate estimates of its age. Similarly,
180 the basis for correlative dates is given, again to facilitate the use of updated estimates of the
181 age of the event. Radiocarbon ages are given in radiocarbon years, but all other ages are given
182 in calendar years BP using 1950 CE as the reference zero date. Error estimates are given for
183 radiometric ages and wherever possible for calendar ages. We provide an indication of whether
184 a specific date was used in the original age model for the entity, and an explanation for why
185 specific dates were rejected, since this can be a guide as to whether the dates should be
186 incorporated in the construction of new age models. **A list of the valid choices for fields that
187 are selected from a pre-defined list (e.g. material dated) is given in Table S2.**

188

189 Table 4 Definition of the date info table.

Field name	Definition	Data type	Constraints / Notes
ID_DATE_INFO	Unique identifier for the date record	Unsigned integer	Auto-numeric, primary key, a positive integer
ID_ENTITY	Unique identifier for the entity (as in entity table)	Unsigned integer	Auto-numeric, foreign key of the entity table, a positive integer
material_dated	Material from which the date was obtained, if applicable	Text	Selected from pre-defined list
date_type	Technique used to obtain the date measurement	Text	Selected from pre-defined list
avg_depth	Average depth in the sedimentary sequence where the date was measured, in metres	Double	None
thickness	Thickness of the sample used for dating, in metres	Double	None
lab_number	Unique identifying code assigned by the dating laboratory	Text	65,535 characters maximum length
age_C14	Uncalibrated radiocarbon age	Double	None
age_calib	The calendar age of a date	Double	None
error	Analytical or measurement error on the date	Double	None
correlation_info	Indication of basis for correlative dating (e.g. pollen, tephra or stratigraphic correlations)	Text	Selected from pre-defined list
age_used	Indicates whether date was used by the author(s) in the	Text	Selected from pre-defined list

	construction of the original age model		
reason_age_not_used	Indication of why a date was not used in the original age model. Blank if dates were used in original model	Text	Selected from pre-defined list
notes	Additional comments regarding a date record	Text	The maximum length is 65,535 characters

190 **2.2.5 Publication information (table name: publication)**

191 This table provides full bibliographic citations for the original references documenting the
192 charcoal records and/or their age models. There may be multiple publications for a single
193 charcoal record, and all of these references are listed. Conversely, there may be a single
194 publication for multiple charcoal records. There is also a table (table name:
195 entity_link_publication) that links the publications to the specific entity.

196 **2.2.6 Original age model information (table name: chronology)**

197 This table provides information about the original age model for each record, and the ages
198 assigned to individual samples. There can be many records that use the same type of age model
199 (e.g. linear interpolation, spline, regression), and for convenience, there is a table that links the
200 records to the age model name (table name: model name).

201 **2.2.7 New age model information (table name: age_model)**

202 This table contains information about the age models that have been constructed for this version
203 of the database using the INTCAL2020 calibration curve (Reimer et al., 2020) and the BACON
204 (Blaauw et al., 2021) age modelling R package (see section 2.3). We preserve information on
205 the mean and median ages, as well as the quantile ranges for each sample.

206

207 Table 5 Definition of the age model table.

Field name	Definition	Data type	Constraints / Notes
ID_MODEL	Unique identifier for the technique used to generate the age model (original age models from existing authors in the chronology table, and new age models in the age_model table)	Unsigned integer	Auto-numeric, composite primary key with ID_SAMPLE, foreign key of the model_name table, positive integer
ID_SAMPLE	Unique identifier for the sample (as in sample table)	Unsigned integer	Auto-numeric, composite primary key with ID_MODEL, foreign key of the sample table, positive integer
mean	Mean age of the sample	Integer	None
median	Median age of the sample	Integer	None
UNCERT_5	Lower bound of the 95% confidence interval for the median age	Integer	None
UNCERT_95	Upper bound of the 95% confidence interval for the median age	Integer	None
UNCERT_25	Lower bound of the 75% confidence interval for the median age	Integer	None
UNCERT_75	Upper bound of the 75% confidence interval for the median age	Integer	None

208 **2.3 Construction of new age models**

209 The original age models for the charcoal records were made at different times, using different
 210 radiocarbon calibration curves, and using different age-modelling methods. We standardised

211 the age modelling, using RBacon (Blaauw and Christen, 2011; Blaauw et al., 2021) to construct
212 new Bayesian age-depth models in the ageR package (Villegas-Diaz et al., 2021). The ageR
213 package provides functions that facilitate the supervised creation of multiple age models for
214 many cores and different data sources, including databases, comma and tab separated files. The
215 INTCAL20 Northern Hemisphere calibration curve (Reimer et al., 2020) and the SHCAL20
216 Southern Hemisphere calibration curve (Hogg et al., 2020) were used for entities between the
217 latitudes of 90° and 15°N and 15 to 90°S respectively. Entities in equatorial latitudes (15°N to
218 15°S) used a 50:50 mixed calibration curve to account for north-south air mass-mixing
219 following Hogg et al. (2020), and radiocarbon ages from marine entities were calibrated using
220 the Marine20 calibration curve (Heaton et al., 2020).

221 To estimate the optimum age modelling scenarios based upon the date and sample information
222 for each entity, multiple RBacon age models were run using different *prior* accumulation rate
223 (acc.mean) and thickness values. *Prior* accumulation rate values were selected using an initial
224 linear regression of the ages in each entity, which was then increased (decreased) sequentially
225 from the default value up to twice more (less) than the initial value. As an example, if the initial
226 accumulation rate value selected from the linear regression was 20 yr/cm, age models would
227 also be run using values of 10, 15, 20, 30 and 40 yr/cm. In cases where the regional
228 accumulation rate was known, the upper and lower values of the accumulation rate scenarios
229 were manually constrained. The range of *prior* thicknesses used in the models were calculated
230 by increasing and decreasing the RBacon default thickness value (5 cm) up to a value one
231 eighth of the overall length of the core. For a 400 cm core for example, the thickness scenarios
232 would be 5, 10, 15, 20, 25, 30, 35, 40, 45 and 50 cm. Thus, the number of scenarios created by
233 possible accumulation rates and thicknesses varies between different entities. Depths of known
234 hiatuses reported in the original publications were included in the date info table (section 2.2.4)
235 and have also been included in the age models run in ageR. In instances where the
236 sedimentation rates were different above and below an hiatus, separate age models were run
237 before and after the non-deposition period to account for these variations (Blaauw and Christen,
238 2011).

239 A three-step procedure was used to select the best model for each entity. First, an optimum
240 model was selected by ageR, using the lowest quantified area between the *prior* and *posterior*
241 accumulation rate distribution curves (Supplementary Figure 1). This selection was checked
242 manually using comparisons between the distance of the estimated ages and the controls to

243 check the accuracy of the model interpolation. Finally, the age model was visually inspected
244 to ensure that final interpolation accurately represented the date information and did not show
245 abrupt shifts in accumulation rates or changes at the dated depths. If the ageR model selection
246 was deemed to be erroneous or inaccurate, the next suitable model with the lowest area between
247 the *prior* and *posterior* curves, which accurately represented the distribution of dates in the
248 sequence, was selected (Supplementary Figure 2).

249 **2.4 Quality control**

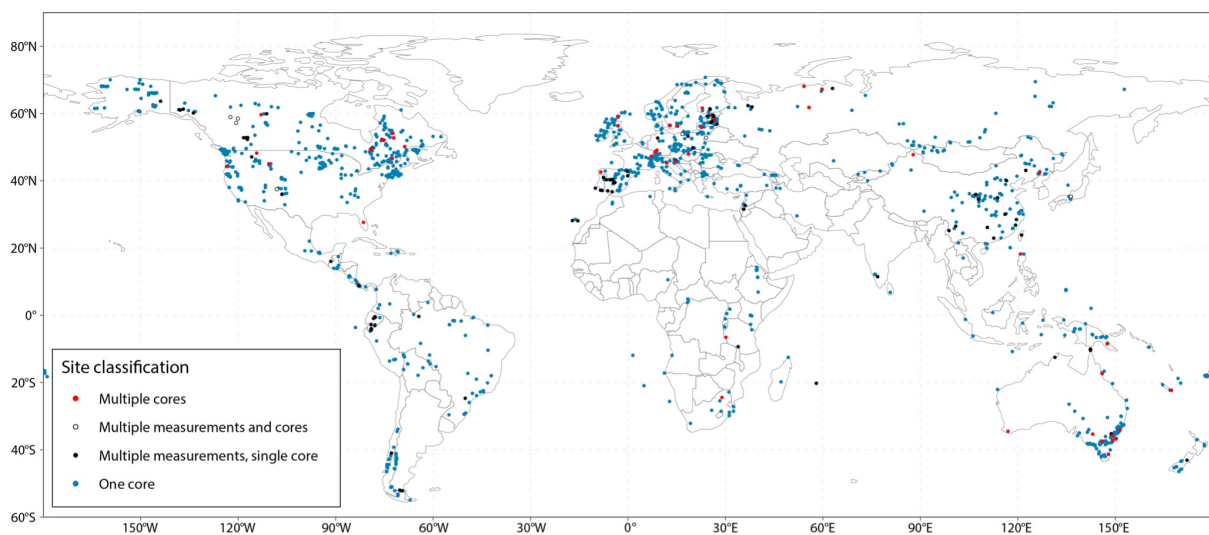
250 Individual records in the RPD were compiled either by the original authors or from published
251 and open-access material by specialists in the collection and interpretation of charcoal records.
252 Records that were obtained from published and open-access material were cross-checked
253 against publications or with the original authors of those publications whenever possible. Null
254 values for metadata fields were identified during the initial checking procedure, and checks
255 were made with the data contributors to determine whether these genuinely corresponded to
256 missing information. In the database, null values are reserved for fields where the required
257 information is not applicable, for example water depth for terrestrial sites or laboratory sample
258 numbers for correlative dates. We distinguish fields where information could be available but
259 was never recorded or has subsequently been lost (represented by -999999), and fields where
260 we were unable to obtain this information but it could be included in subsequent updates of the
261 database (represented by -777777). We also distinguish fields where specific metadata is not
262 applicable (represented by -888888), for example basin size for a marine core or water depth
263 for a terrestrial small hollow.

264 Prior to entry in the database, the records were automatically checked using specially designed
265 database scripts (in R) to ensure that the entries to individual fields were in the format expected
266 (e.g. text, decimal numeric, positive integers) or were selected from the pre-defined lists
267 provided for specific fields. Checks were also performed to find duplicated rows (e.g.
268 duplicated sampling depths within the same entity).

269 **3. Overview of database contents**

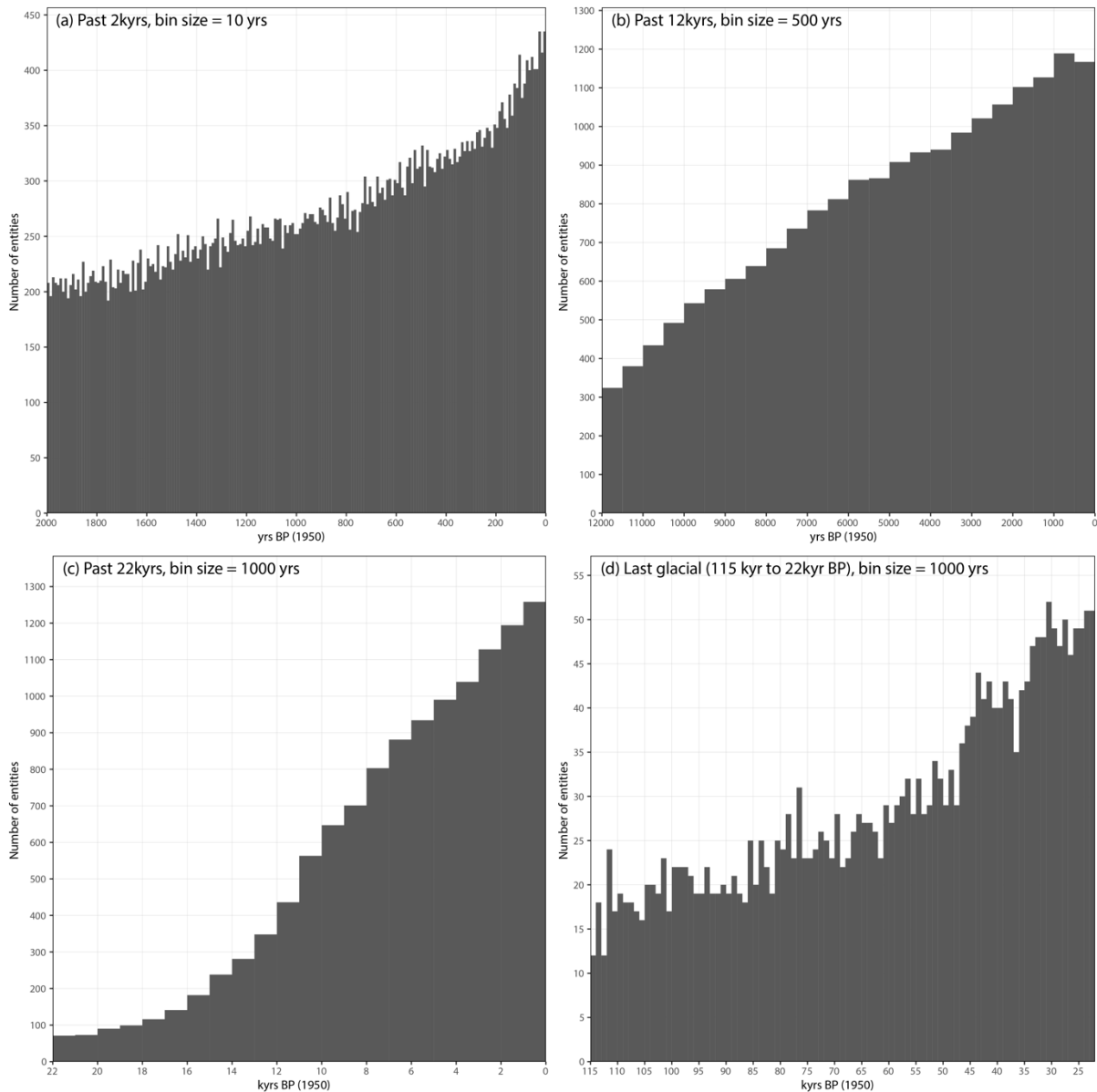
270 This first version of the RPD contains 1676 individual charcoal records from 1480 sites
271 worldwide. This represents a 128% increase compared to the number of records in version 3

272 of the Global Charcoal Database (GCDv3: Marlon et al., 2016; 736 records) and a 79% increase
 273 compared to version 4 (Blarquez, 2018; 935 records) and a 36% increase compared to the
 274 online version of the GCD (1232 records). The RPD includes 840 records that are not available
 275 in any version of the GCD, and provides updated or corrected information for a further 485
 276 records that were included in the GCD. Raw data are available for 14% of the entities and
 277 concentration for 67% of the entities; influx based on the original age models is given for 16%
 278 of the entities. The original age models for 67 (4%) of the records included in the RPD were
 279 derived solely by layer counting, U/Th or Pb dates, or isotopic correlation and therefore are
 280 already expressed in calendar ages. However, we have provided new age models for 22 of these
 281 records (33%), where the dates or correlations points were specified, using the supervised age
 282 modelling procedure for consistency. New age models have been created for 807 (50%) of the
 283 remaining charcoal records where the original chronology was based on radiometric dating.
 284 The geographic coverage of the RPD (Figure 2) is biased towards the northern extratropics.
 285 However, there is a growing representation of records from China, the Neotropics (Central and
 286 South America), southern and eastern Africa, and eastern Australia. The largest gaps
 287 geographically are in currently dry regions, which often lack sites with anoxic sedimentation
 288 suitable for the preservation of charcoal and are generally under-represented in palaeofire
 289 reconstructions (Leys et al., 2018). The temporal coverage of the records is excellent for the
 290 interval since 22,000 years ago, with 774 records with a minimum resolution of 10 years for
 291 the past 2000 years, 1335 records with a minimum resolution of 500 years for the past 12,000
 292 years, and 1382 records with a minimum resolution of 1000 years for the past 22,000 years.
 293 There are fewer records for earlier intervals. Nevertheless, there are 70 records that provide
 294 evidence for the interval of the last glacial period before the Last Glacial Maximum (22-115
 295 ka) including the response of fire to rapid climate warmings (Dansgaard-Oeschger events).



296

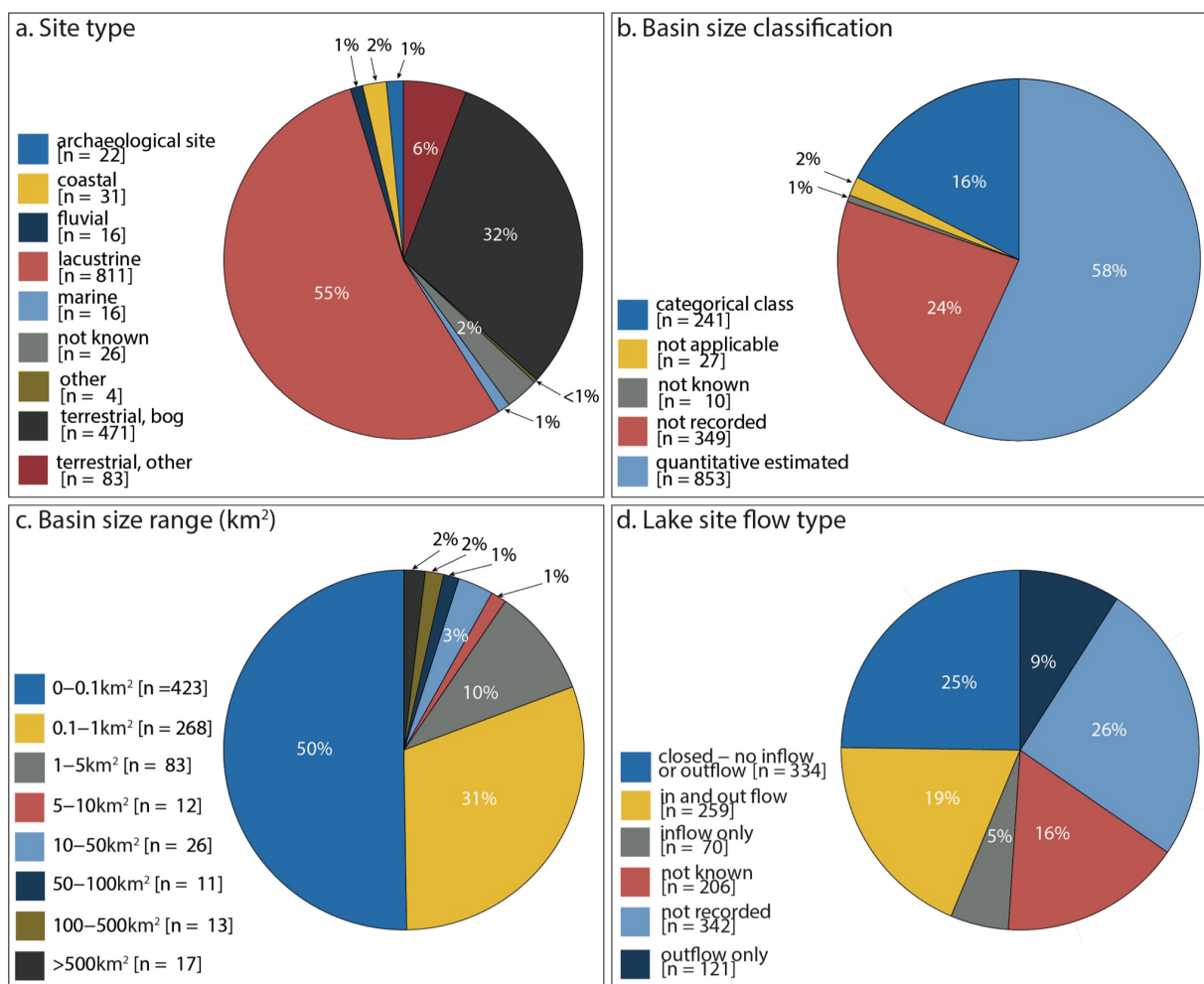
297 *Figure 2. Map showing the location of sites included in the RPD. As shown here, some sites*
 298 *have multiple records, either representing separate cores from the same hydrological basin or*
 299 *representing measurements of different charcoal size fractions on the same core. These records*
 300 *are treated as separate entities in the database itself.*
 301



302 *Figure 3. Plot showing the temporal coverage of individual entities in the database. Panel (a)*
 303 *shows records covering the past 2000 years (2kyrBP), (b) shows records covering the past*
 304 *12,000 years, (c) for the past 22 000 years (22 kyr BP) and thus encompassing the Last Glacial*
 305 *Maximum. (LGM), and (d) shows records that cover the interval of the last glacial prior to the*
 306 *LGM (22–115 kyr BP).*
 307

308 Information about site type (Figure 4a) is included in the database because this could influence
 309 whether the charcoal is of local origin or represents a more regional palaeofire signal. For
 310 example, records from small forest hollows provide a very local signal of fire activity and
 311 records from peat bogs most likely sample fires on the peatland itself, whereas records from

312 lakes could provide both local and regional fire signals. More than half (55%) of the records in
 313 the RPD are derived from lakes (811 entities). Records from peatlands are also well represented
 314 (471 entities, 32%). Basin size, particularly in the case of lakes, influences the source area for
 315 charcoal particles transported by wind. However, the existence of inflows and outflows to the
 316 system can also affect the charcoal record. Quantitative information is now available for more
 317 than half of the lake sites (Figure 4b), and most (691 sites, 81%) of the records (Figure 4c) are
 318 from relatively small lakes (<1 km²). A quarter of the charcoal records from lakes (Figure 4d)
 319 are from closed basins (334 sites).



320
 321 *Figure 4. Availability of metadata that can be used to select suitable sites for specific analyses*
 322 *or for quality control. Plot (a) shows the distribution of sites by type. Some site types have finer*
 323 *distinctions recorded in the database: lacustrine environments, for example, are sub-divided*
 324 *according to origin. Plot (b) shows the number of sites with quantitative estimates versus*
 325 *categorical assessments of basin size and plot (c) shows the number of sites in specific basin*
 326 *size ranges. Plot (d) shows the distribution of different hydrological types for lake records.*

327 **4. Data availability**

328 Version 1 of the Reading Palaeofire Database (RPDv1b: Harrison et al., 2021, doi:
329 [10.17864/1947.000345](https://doi.org/10.17864/1947.000345)) is available in SQL format from
330 <https://doi.org/10.17864/1947.000345>. The individual tables are also available as csv files. The
331 R package used to create the new age models is available from [https://github.com/special-](https://github.com/special-uor/ageR)
332 [uor/ageR](https://github.com/special-uor/ageR) (Villegas-Diaz et al., 2021).

333 **5. Conclusions**

334 The Reading Palaeofire Database (RPD) is an effort to improve the coverage of charcoal
335 records that can be used to investigate palaeofire regimes. New age models have been
336 developed for 48% of the records to take account of recent improvements in radiocarbon
337 calibration and age modelling methods. In addition to expanded coverage and improved age
338 models, considerable effort has been made to include metadata and quality control information
339 to allow the selection of records appropriate to address specific questions and to document
340 potential sources of uncertainty in the interpretation of the records. The first version of the RPD
341 contains 1676 individual charcoal records (entities) from 1480 sites worldwide. Geographic
342 coverage is best for the northern extratropics, but the coverage is good except for semi-arid and
343 arid regions. Temporal coverage is good for the past 2000 years, the Holocene and back to the
344 LGM, but there is a reasonable number of longer records. The database is publicly available,
345 both as an SQL database and as csv files.

346 **Author contributions.** SPH and RV-D designed the database; RV-D, DK, PL and SPH were
347 responsible for construction of the database; A-LD advised on incorporation of data from the
348 GCD and the standardisation of charcoal units; EC-S, DG, DK, PL, YS, LS provided updated
349 age models; the other authors provided original data or metadata and quality control on
350 individual records; SPH wrote the first draft of the paper and all authors contributed to the final
351 draft.

352 **Competing Interests.** The authors declare that they have no conflict of interest.

353 **Acknowledgements.** RV-D, SPH, EC-S, and YS acknowledge support from the ERC-funded
354 project GC2.0 (Global Change 2.0: Unlocking the past for a clearer future, grant number

355 694481). SPH, PL, DG, DK, LS acknowledge support from the Leverhulme Centre for
356 Wildfires, Environment and Society through the Leverhulme Trust, grant number RC-2018-
357 023. AF acknowledges support from the German Research Foundation (grant no. FE-1096/6-
358 1). KM acknowledges support from the Swiss Government Excellence Postdoctoral
359 Scholarship (grant no. FIRECO 2016.0310); the National Science Centre in Poland (grant no.
360 2015/17/B/ST10/01656); grant PSPB-013/2010 from Switzerland through the Swiss
361 Contribution to the enlarged European Union; the Scientific Exchange Programme from the
362 Swiss Contribution to the New Member States of the European Union (Sciex-NMS ch) –
363 SCIEX Scholarship Fund, project RE-FIRE 12.286. OL acknowledges support from the
364 Mobilitas Plus post-doctoral research grant of The Estonian Research Council (MOBJD313).
365 We would like to thank our many colleagues from the PAGES Global Palaeofire Working
366 Group for their contributions to the construction of the Global Charcoal Database which
367 provided the starting point for the current compilation, and our colleagues from the Leverhulme
368 Centre for Wildfires, Environment and Society for discussions of the use of palaeodata to
369 reconstruct past fire regimes. We thank Manfred Rösch for providing information on dating
370 for several sites. **We also thank Dan Gavin and Jack Williams for helpful reviews of the original**
371 **manuscript.**
372

373 **References**

- 374 **Abatzoglou, J. T., and Williams, A. P.: Impact of anthropogenic climate change on wildfire**
375 **across western US forests, *Proceedings of the National Academy of Sciences*, 113,**
376 **11,770–11,775, <https://doi.org/10.1073/pnas.1607171113>, 2016.**
- 377 **Andela, N., Morton, D. C., Giglio, L., Paugam, R., Chen, Y., Hanson, S., van der Werf, G. R.,**
378 **and Randerson, J. T.: The Global Fire Atlas of individual fire size, duration, speed, and**
379 **direction, *Earth System Science Data*, 11, 529–552, [https://doi.org/10.5194/essd-11-](https://doi.org/10.5194/essd-11-529-2019)**
380 **529-2019, 2019.**
- 381 Arora, V. K. and Melton, J. R.: Reduction in global area burned and wildfire emissions since
382 1930s enhances carbon uptake by land, *Nat. Commun.*, 9, 1326,
383 <https://doi.org/10.1038/s41467-018-03838-0>, 2018.
- 384 Bistinas, I., Harrison, S. P., Prentice, I. C., and Pereira, J. M. C.: Causal relationships vs.
385 emergent patterns in the global controls of fire frequency, *Biogeosci.*, 11, 5087-5101,
386 2014.
- 387 Blaauw, M. J. Christen, A.: Flexible paleoclimate age-depth models using an autoregressive
388 gamma process, *Bayesian Analysis*, 6, 457-474, <https://doi.org/10.1214/11-BA618>,
389 2011.
- 390 Blaauw, M., Christen, J. A., Aquino Lopez, M.A., Esquivel Vazquez, J., Gonzalez, O.M.,
391 Belding, T., Theiler, J., Gough, B., Karney, C.: rbacon: Age-Depth Modelling using
392 Bayesian Statistics, <https://CRAN.R-project.org/package=rbacon>, 2021.
- 393 Blarquez, O.: GCD, <https://CRAN.R-project.org/package=GCD>, 2018.
- 394 Blarquez, O., Vanni ere, B., Marlon, J. R., Daniau, A-L., Power, M. J., Brewer, S. and Bartlein,
395 P. J. paleofire: An R package to analyse sedimentary charcoal records from the Global
396 Charcoal Database to reconstruct past biomass burning, *Computers & Geosci.*, 72, 255-
397 261, <https://doi.org/10.1016/j.cageo.2014.07.020>, 2014.
- 398 Bond, W. J., Woodward, F. I., and Midgley, G. F.: The global distribution of ecosystems in a
399 world without fire, *New Phytol.*, 165, 525–538, 2005.
- 400 Bowman, D. M. J. S., Perry, G. L. W., Higgins, S. I., Johnson, C. N., Fuhlendorf, S. D., and
401 Murphy, B. P.: Pyro- diversity is the coupling of biodiversity and fire regimes in food
402 webs, *Philos. T. R. Soc. Lond.*, 371, 20150169, <https://doi.org/10.1098/rstb.2015.0169>,
403 2016.
- 404 **Clark, J. S., and Patterson, W. A.: Background and local charcoal in sediments: Scales of fire**
405 **evidence in the paleorecord, in: *Sediment Records of Biomass Burning and Global***

406 Change. Springer Berlin Heidelberg, Berlin, Heidelberg, pp. 23–48.
407 https://doi.org/10.1007/978-3-642-59171-6_3, 1997.

408 Conedera, M., Tinner, W., Neff, C., Meurer, M., Dickens, A.F., and Krebs, P.: Reconstructing
409 past fire regimes: methods, applications, and relevance to fire management and
410 conservation, *Quaternary Science Reviews*, 28, 555–576,
411 <https://doi.org/10.1016/j.quascirev.2008.11.005>, 2009.

412 Daniau, A.-L., Bartlein, P. J., Harrison, S. P., Prentice, I. C., Brewer, S., Friedlingstein, P.,
413 Harrison-Prentice, T. I., Inoue, J., Marlon, J. R., Mooney, S., Power, M. J., Stevenson,
414 J., Tinner, W., Andrič, M., Atanassova, J., Behling, H., Black, M., Blarquez, O., Brown,
415 K. J., Carcaillet, C., Colhoun, E., Colombaroli, D., Davis, B. A. S., D’Costa, D.,
416 Dodson, J., Dupont, L., Eshetu, Z., Gavin, D. G., Genries, A., Gebru, T., Haberle, S.,
417 Hallett, D. J., Horn, S., Hope, G., Katamura, F., Kennedy, L., Kershaw, P., Krivonogov,
418 S., Long, C., Magri, D., Marinova, E., McKenzie, G. M., Moreno, P. I., Moss, P.,
419 Neumann, F. H., Norström, E., Paitre, C., Rius, D., Roberts, N., Robinson, G., Sasaki,
420 N., Scott, L., Takahara, H., Terwilliger, V., Thevenon, F., Turner, R. B., Valsecchi, V.
421 G., Vannière, B., Walsh, M., Williams, N., and Zhang, Y.: Predictability of biomass
422 burning in response to climate changes, *Glob. Biogeochem. Cyc.*, 26, GB4007,
423 [doi:10.1029/2011GB004249](https://doi.org/10.1029/2011GB004249), 2012.

424 Daniau, A.-L., Harrison, S. P., and Bartlein, P. J.: Fire regimes during the last glacial, *Quat.*
425 *Sci. Rev.*, 29: 2918-2930, 2010.

426 Dutta, R., Das, A., and Aryal, J.: Big data integration shows Australian bush-fire frequency is
427 increasing significantly, *Royal Society Open Science*, 3, [10.1098/rsos.150241](https://doi.org/10.1098/rsos.150241), 2016.

428 Evangeliou, N., Kylling, A., Eckhardt, S., Myroniuk, V., Stebel, K., Paugam, R., Zibitsev, S.,
429 and Stohl, A.: Open fires in Greenland in summer 2017: transport, deposition and
430 radiative effects of BC, OC and BrC emissions, *Atmospheric Chemistry and Physics*,
431 19, 1393-1411, [10.5194/acp-19-1393-2019](https://doi.org/10.5194/acp-19-1393-2019), 2019.

432 Forkel, M., Dorigo, W., Lasslop, G., Teubner, I., Chuvieco, E., and Thonicke, K.: A data-
433 driven approach to identify controls on global fire activity from satellite and climate
434 observations (SOFIA V1), *Geosci. Model Dev.*, 10, 4443–4476,
435 <https://doi.org/10.5194/gmd-10-4443-2017>, 2017.

436 Forkel, M., Andela, N., Harrison, S. P., Lasslop, G., van Marle, M., Chuvieco, E., Dorigo, W.,
437 Forrest, M., Hantson, S., Heil, A., Li, F., Melton, J., Sitch, S., Yue, C., and Arneth, A.:
438 Emergent relationships with respect to burned area in global satellite observations and

439 fire-enabled vegetation models, *Biogeosciences*, 16, 57–76, [https://doi.org/10.5194/bg-](https://doi.org/10.5194/bg-16-57-2019)
440 [16-57-2019](https://doi.org/10.5194/bg-16-57-2019), 2019.

441 Feurdean, A., Vanni ere, B., Finsinger, W., Warren, D., Connor, S. C., Forrest, M., Liakka, J.,
442 Panait, A., Werner, C., Andri , M., Bobek, P., Carter, V. A., Davis, B., Diaconu, A.-
443 C., Dietze, E., Feeser, I., Florescu, G., Ga ka, M., Giesecke, T., Jahns, S., Jamrichova,
444 E., Kajuka o, K., Kaplan, J., Karpinska-Ko aczek, M., Ko aczek, P., Kuneš, P.,
445 Kupriyanov, D., Lamentowicz, M., Lemmen, C., Magyari, E. K., Marcisz, K.,
446 Marinova, E., Niamir, A., Novenko, E., Obremaska, M., P edziszewska, A., Pfeiffer, M.,
447 Poska, A., R osch, M., S lowiński, M., Stan ikait e, M., Szal, M., Świ eta-Musznicka, J.,
448 Tan au, I., Theuerkauf, M., Tonkov, S., Valk o, O., Vassiljev, J., Veski, S., Vincze, I.,
449 Wacnik, A., Wiethold, J., Hickler, T.: Fire hazard modulation by long-term dynamics
450 in land cover and dominant forest type in eastern and central Europe, *Biogeosci.*, 17,
451 1213-1230, [10.5194/bg-17-1213-2020](https://doi.org/10.5194/bg-17-1213-2020), 2020.

452 Harrison, S. P., Bartlein, P. J., Brovkin, V., Houweling, S., Kloster, S., and Prentice, I. C.:
453 Biomass burning contribution to global climate-carbon cycle feedback, *Earth System*
454 *Dyn.*, 9, 663-67, <https://doi.org/10.5194/esd-9-663-2018>, 2018.

455 Harrison, S. P., Marlon, J. R., Bartlein, P. J.: Fire in the Earth System, In *Changing Climates,*
456 *Earth Systems and Society International Year of Planet Earth*, pp 21-48. Springer
457 Publisher, 2010.

458 Harrison, S.P., Villegas-Diaz, R., Lincoln, P., Kesner, D., Cruz-Silva, E., Sweeney, L., Shen,
459 Y. and Gallagher, D.: The Reading Palaeofire Database: an expanded global resource
460 to document changes in fire regimes from sedimentary charcoal records. University of
461 Reading Dataset. <http://dx.doi.org/10.17864/1947.319>;
462 <https://researchdata.reading.ac.uk/id/eprint/319>, 2021

463 Hayasaka, H.: Rare and extreme wildland fire in Sakha in 2021, *Atmosphere*, 12, 1572.
464 <https://doi.org/10.3390/atmos12121572>, 2021.

465 He, T., Lamont, B. B., and Pausas, J. G.: Fire as a key driver of Earth's biodiversity, *Biol. Rev.*,
466 94, 1983–2010, <https://doi.org/10.1111/brv.12544>, 2019.

467 Heaton, T., K ohler, P., Butzin, M., Bard, E., Reimer, R., Austin, W., Bronk Ramsey, C.,
468 Grootes, P. M., Highen, K. A., Kromer, B., Reimer, P. J., Adkins, A., Burke, A. M.,
469 Cook, M. S., Olsen, J., and Skinner, L.: Marine 20 — The marine radiocarbon age
470 calibration curve (0-55,000 cal BP), *Radiocarbon*, 62, 779-820, doi:
471 [10.1017/RDC.2020.68](https://doi.org/10.1017/RDC.2020.68), 2020.

472 Hogg, A., Heaton, T., Hua, Q., Palmer, J., Turney, C., Southon, J., Bayliss, A., Blackwell, P.
473 G., Boswijk, G., Bronk Ramsey, C., Pearson, C., Petchey, F., Reimer, P., Reimer, R.,
474 and Wacker, L.: SHCal 20 southern Hemisphere calibration, 0-55,000 years cal BP,
475 *Radiocarbon*, 62, 759-778, doi: 10.1017/RDC.2020.59, 2020.

476 Knorr, K., Jiang, L. and Arneth, A.: Climate, CO₂, and demographic impacts on global wildfire
477 emissions, *Biogeosci.*, 12, 267-282, 10.5194/bg-12-15011-2015, 2016.

478 Lasslop, G., Coppola, A. I., Voulgarakis, A., Yue, C., and Veraverbeke, S.: Influence of fire
479 on the carbon cycle and climate, *Current Clim. Change Rep.*, 5, 112–123,
480 <https://doi.org/10.1007/s40641-019-00128-9>, 2019.

481 Lasslop, G., Hantson, S., Harrison, S. P., Bachelet, D., Burton, C., Forkel, M., Forrest, M., Li,
482 F., Melton, J. R., Yue, C., Archibald, S., Scheiter, S., Arneth, A., Hickler, T., and Sitch,
483 S.: Global ecosystems and fire: multi-model assessment of fire-induced tree cover and
484 carbon storage reduction, *Global Change Biology*, 26, 5027-5041, 10.1111/gcb.15160,
485 2020.

486 Leys, B., Marlon, J.R., Umbanhowar, C., Vanniere, B.: Global fire history of grassland biomes.
487 *Ecology and Evolution* 8 (17), 8831-8852, 2018.

488 Li, F., Bond-Lamberty, B., Levis, S.: Quantifying the role of fire in the Earth system—Part 2:
489 Impact on the net carbon balance of global terrestrial ecosystems for the 20th century,
490 *Biogeosciences*, 11, 1345–1360, 2014.

491 Li, F., Lawrence, D. M., and Bond-Lamberty, B.: Impact of fire on global land surface air
492 temperature and energy budget for the 20th century due to changes within
493 ecosystems, *Environmental Research Letters*, 12, 044014, 2017.

494 Li, F., Val Martin, M., Andreae, M. O., Arneth, A., Hantson, S., Kaiser, J. W., Lasslop, G.,
495 Yue, C., Bachelet, D., Forrest, M., Kluzek, E., Liu, X., Mangeon, S., Melton, J. R.,
496 Ward, D. S., Darmenov, A., Hickler, T., Ichoku, C., Magi, B. I., Sitch, S., van der Werf,
497 G. R., Wiedinmyer, C., and Rabin, S. S.: Historical (1700–2012) global multi-model
498 estimates of the fire emissions from the Fire Modeling Intercomparison Project
499 (FireMIP), *Atmospheric Chemistry and Physics*, 19, 12545–12567,
500 <https://doi.org/10.5194/acp-19-12545-2019>, 2019.

501 Liu, Z., Ballantyne, A. P., and Cooper, L. A.: Biophysical feedback of global forest fires on
502 surface temperature, *Nature Communications*, 10, 214,
503 <https://doi.org/10.1038/s41467-018-08237-z>, 2019.

504 Marlon, J., Bartlein, P. J., Carcaillet, C., Gavin, D. G., Harrison, S. P., Higuera, P. E., Joos, F.,
505 Power, M., and Prentice, I. C.: Climate and human influences on global biomass

506 burning over the past two millennia, *Nature Geosciences*, 1, 697-702, doi:
507 10.1038/ngeo313, 2008.

508 Marlon, J.R., Bartlein, P. J., Daniau, A-L., Harrison, S. P., Power, M. J., Tinner, W.,
509 Maezumie, S., and Vanni re, B.: Global biomass burning: A synthesis and review of
510 Holocene paleofire records and their controls, *Quaternary Science Reviews*, 65, 5-25,
511 2013.

512 Marlon, J.R, Bartlein, P. J., Long, C., Gavin, D. G., Anderson, R. S., Briles, C., Brown, K.,
513 Colombaroli, D., Hallett, D. J., Power, M. J., Scharf, E., and Walsh, M. K.: Long-term
514 perspective on wildfires in the western U.S.A., *Proceeding of the National Academy of*
515 *Sciences*, 109, E535-E543, <https://doi.org/10.1073/pnas.1112839109>, 2012.

516 Marlon, J. R., Bartlein, P. J., Walsh, M. K., Harrison, S. P., Brown, K. J., Edwards, M. E.,
517 Higuera, P. E., Power, M. J., Anderson, R. S., Briles, C., Brunelle, A., Carcaillet, C.,
518 Daniels, M., Hu, F. S., Lavoie, M., Long, C., Minckley, T., Richard, P. J. H., Scott, A.
519 C., Shafer, D. S., Tinner, W., Umbanhower, C. E. Jr., and Whitlock, C.: Wildfire
520 responses to abrupt climate change in North America, *Proceeding of the National*
521 *Academy of Sciences*, 106, 2519-2524, doi: 0.1073/pnas.0808212106, 2009.

522 Marlon. J., Bartlein, P. J., and Whitlock, C.: Fire-fuel-climate linkages in the northwestern
523 USA during the Holocene, *Holocene*, 16,1059–1071, 2006.

524 Marlon, J. R., Kelly, R., Daniau, A.-L., Vanni re, B., Power, M. J., Bartlein, P. J., Higuera,
525 P., Blarquez, O., Brewer, S., Br ucher, T., Feurdean, A., Romera, G. G., Iglesias, V.,
526 Maezumi, S. Y., Magi, B., Courtney Mustaphi, C. J., and Zhihai, T.: Reconstructions
527 of biomass burning from sediment charcoal records to improve data-model
528 comparisons, *Biogeosciences*, 13, 3325–3244, doi:10.5194/bg-13-3225-2016, 2016.

529 Mooney, S., Harrison, S. P., Bartlein, P. J., Daniau A.-L., Stevenson, J., Brownlie, K.,
530 Buckman, S., Cupper, M., Luly, J., Black, M., Colhoun, E., D’Costa, D., Dodson, J.,
531 Haberle, S., Hope, G. S., Kershaw, P., Kenyon, C., McKenzie., M., Williams, N.: Late
532 Quaternary fire regimes of Australasia, *Quaternary Science Reviews*, 30, 28-46, 2011.

533 Nolan, R. H. Boer, M. M., Collins, L., Resco de Dios, V., Clarke, H., Jenkins, M., Kenny, B.,
534 and Bradstock, R. A.: Causes and consequences of eastern Australia's 2019–20 season
535 of mega-fires, *Global Change Biology*, 26: 1039-1041, doi:10.1111/gcb.14987, 2020.

536 Pellegrini, A. F. A., Ahlstr m, A., Hobbie, S. E., Reich, P. B., Nieradzik, L. P., Staver, A.
537 C., Scharenbroch, B. C., Jumpponen, A., William R. L. Anderegg, W. R. L., James T.
538 Randerson, J. T., and Jackson, R. B.: Fire frequency drives decadal changes in soil

539 carbon and nitrogen and ecosystem productivity, *Nature*, 553, 194–198.
540 <https://doi.org/10.1038/nature24668>, 2018.

541 Power, M. J., Mayle, F. E., Bartlein, P. J., Marlon, J. R., Anderson, R. S., Behling, H., Brown,
542 K. J., Carcaillet, C., Colombaroli, D., Gavin, D. G., Hallett, D. J., Horn, S. P., Kennedy,
543 L. M., Lane, C. S., Long, C. J., Moreno, P. I., Paitre, C., Robinson, G., Taylor, Z., and
544 Walsh, M. K.: 16th Century burning decline in the Americas: population collapse or
545 climate change? *Holocene*, 1-11, 2013.

546 Power, M. J., Marlon, J. R., Bartlein, P. J., and Harrison, S. P.: Fire history and the Global
547 Charcoal Database: a new tool for hypothesis testing and data exploration, *Palaeogeog.*,
548 *Palaeoclim.*, *Palaeoecol.*, 291, 52-59. doi: 10.1016/j.palaeo.2009.09.014, 2010.

549 Power, M. J., Ortiz, N., Marlon, J., Bartlein, P. J., Harrison, S. P., Mayle, F., Ballouche, A.,
550 Bradshaw, R., Carcaillet, C., Cordova, C., Mooney, S., Moreno, P., Prentice, I. C.,
551 Thonicke, K., Tinner, W., Whitlock, C., Zhang, Y., Zhao, Y., Anderson, R. S., Beer,
552 R., Behling, H., Briles, C., Brown, K., Brunelle A., Bush, M., Clark, J., Colombaroli,
553 D., Chu, C. Q., Daniels, M., Dodson, J., Edwards, M. E., Fisinger, W., Gavin, D. G.,
554 Gobet, E., Hallett, D. J., Higuera, P., Horn, S., Inoue, J., Kaltenrieder, P., Kennedy, L.,
555 Kong, Z. C., Long, C., Lynch, J., Lynch, B., McGlone, M., Meeks, S., Meyer, G.,
556 Minckley, T., Mohr, J., Noti, R., Pierce, J., Richard, P., Shuman, B. J., Takahara, H.,
557 Toney, J., Turney, C., Umbanhower, C., Vandergoes, M., Vanniere, B., Vescovi, E.,
558 Walsh, M., Wang, X., Williams, N., Wilmshurst, J., Zhang, J. H.: Changes in fire
559 activity since the LGM: an assessment based on a global synthesis and analysis of
560 charcoal data, *Clim. Dyn.*, 30: 887-907, doi: 10.1007/s00382.00.0334x, 2008.

561 Power, M. J., Whitlock, C., Bartlein, P. J., and Stevens, L.R.: Fire and vegetation history during
562 the last 3800 years in northwestern Montana, *Geomorph.*, 75, 420–436, 2006.

563 Power, M., Mayle, F., Bartlein, P., Marlon, J.R., Anderson, R.S., Behling, H., Brown, K.J.
564 Carcailler, C., Colombaroli, D., Gavin, D.G., Hallett, D.J., Horn, S.P., Kennedy, L.M.,
565 Lane, C.S., Long, C.J., Moreno, P.I., Paitre, C., Robinson, G., Taylor, Z., Walsh, M.K.:
566 Climatic control of the biomass-burning decline in the Americas after ad 1500. *The*
567 *Holocene*, 23, 3-13, doi:[10.1177/0959683612450196](https://doi.org/10.1177/0959683612450196), 2013.

568 Randerson, J. T., Liu, H., Flanner, M. G., Chambers, S. D., Jin, Y., Hess, P. G., Pfister, G.,
569 Mack, M. C., Treseder, K. K., Welp, L. R., Chapin, F. S., Hardeb, J. W., Goulden, M.L.
570 Lyons, E., Neff, J. C., Schuur, E. A. G., and Zender, C. S.: The impact of boreal forest
571 fire on climate warming, *Science*, 314, 1130–1132, 2006.

- 572 Reimer, P., Austin, W., Bard, E., Bayliss, A., Blackwell, P., Bronk Ramsey, C., Butzin, M.,
573 Cheng, H. Edwards, R.L., Friedrich, M., Grootes, P.M., Guilderson, T.P., Hajdas, I.,
574 Heaton, T.J., Hogg, A.G., Hughen, K.A., Kromer, B., Manning, S.W., Muscheler, R.,
575 Palmer, J.G., Pearson, C., van der Plicht, J., Reimer, R.W., Richards, D.A., Scott, E.M.,
576 Southon, J.R., Turney, C.S.M., Wacker, L., Adolphi, F., Buntgen, U., Capano, M.,
577 Fahrni, S.M., Fogtman-Schulz, A., Friedrich, R., Kohler, P. Kudsk, S., Miyake, F.,
578 Olsen, J., Reinig, F., Sakamoto, M., Sookdeo, M., Talamo, S.: The INTCAL20
579 Northern Hemisphere radiocarbon age calibration curve (0-55 calkBP), *Radiocarbon*,
580 62, 725-757, doi: 10.1017/RDC.2020.21, 2020.
- 581 Rubino, M., D’Onofrio, A., Seki, O., and Bendle, J. A.: Ice- core records of biomass burning,
582 *Anthrop. Rev.*, 3, 140–162, <https://doi.org/10.1177/2053019615605117>, 2016.
- 583 Sokolik, I. N., Soja, A. J., DeMott, P. J., and Winker, D.: Progress and challenges in
584 quantifying wildfire smoke emissions, their properties, transport, and atmospheric
585 impacts. *J. Geophys. Res: Atmos.*, 124, 13005-12025,
586 <https://doi.org/10.1029/2018JD029878>, 2019.
- 587 van der Werf, G. R., Randerson, J. T., Giglio, L., Collatz, G. J., Mu, M., Kasibhatla, P. S.,
588 Morton, D. C., DeFries, R. S. Jin, Y., and van Leeuwen, T. T.: Global fire emissions
589 and the contribution of deforestation, savanna, forest, agricultural, and peat fires (1997–
590 2009). *Atmos. Chem. Physics*, 10, 11707–11735. [https://doi.org/10.5194/acp-10-](https://doi.org/10.5194/acp-10-11707-2010)
591 [11707-2010](https://doi.org/10.5194/acp-10-11707-2010), 2010.
- 592 Vanni re, B., Power, M. J., Roberts, N., Tinner, W., Carri n, J., Magny, M., Bartlein, P. J., and
593 GPWG contributors: Circum-Mediterranean fire activity and climate changes during
594 the mid Holocene environmental transition (8500-2500 cal yr BP), *Holocene*, 21, 53-
595 73, 2011.
- 596 Villegas-Diaz, R., Cruz-Silva, E., Harrison, S. P. ageR: Supervised Age Models.
597 <https://doi.org/10.5281/zenodo.4636716>, 2021.
- 598 Voulgarakis, A., and Field, R. D. Fire influences on atmospheric composition, air quality and
599 climate, *Curr. Pollution Rep.*, 1, 70–81, <https://doi.org/10.1007/s40726-015-0007-z>,
600 2015.
- 601 Williams, A. N., Mooney, S. D., Sisson, S. A., and Marlon, J. R.: Exploring the relationship
602 between Aboriginal population indices and fire in Australia over the last 20,000 years,
603 *Palaeogeog., Palaeoclim., Palaeoecol.*, 432, 49-57, 2015.
- 604 Williams, A. P., Abatzoglou, J. T., Gershunov, A., Guzman-Morales, J., Bishop, D. A., Balch,
605 J. K., and Lettenmaier, D. P.: Observed impacts of anthropogenic climate change on

606 wildfire in California, *Earth's Future*, 7, 892–910, [https://doi.org/](https://doi.org/10.1029/2019EF001210)
607 [10.1029/2019EF001210](https://doi.org/10.1029/2019EF001210), 2019.